ISBN: 978-3-95450-224-0 ISSN: 2673-7035 doi:10.18429/JACoW-FLS2023-TU1B3

NONLINEAR OPTICS FROM HYBRID DISPERSIVE ORBITS*

Yongjun Li†, Derong Xu, Victor Smaluk, Robert Rainer
Brookhaven National Laboratory, Upton, NY, USA

Abstract

In this paper we present an expansion of the technique of characterizing nonlinear optics from off-energy orbits (NOECO) [Olsson et al., Phys. Rev. Accel. Beams, vol. 23, p. 102803] to cover harmonic sextupoles in storage rings. The existing NOECO technique has been successfully used to correct the chromatic sextupole errors on the MAX-IV machine, however, it doesn't account for harmonic sextupoles, which are widely used on many other machines. Through generating vertical dispersion with chromatic skew quadrupoles, a measurable dependence of nonlinear optics on harmonic sextupoles can be observed from hybrid horizontal and vertical dispersive orbits. Proof of concept of our expanded technique was accomplished by simulations and beam measurements on the National Synchrotron Light Source II (NSLS-II) storage ring.

INTRODUCTION

Characterizing the nonlinear optics of storage rings is becoming more essential with the introduction of higher order multipole magnets in accelerator design. Errors from the higher order multipoles have been observed to degrade machine performance, such as reduction of dynamic aperture, energy acceptance, etc. Some efforts have been made to identify the nonlinear multipole errors by measuring local resonances [1] and distorted resonance driving terms [2], which requires a sophisticated Hamiltonian dynamics analysis. A more practical technique for measuring the nonlinear optics from off-energy closed orbits (NOECO) was reported and demonstrated on the MAX-IV ring [3]. Significant improvements on its dynamic aperture and beam lifetime were observed after correcting sextupole errors. Desired results were obtained while testing the NOECO technique on the ESRF-EBS ring as well [4]. However, the dependence of nonlinear optics on off-energy orbits is only measurable for chromatic sextupoles. This technique, however, doesn't apply to harmonic sextupoles, which do not see the first order linear dispersion. Harmonic sextupoles are used in almost every third-generation light source ring, and some fourth-generation diffraction-limited machines, such as the ALS-U ring [5]. They are even being used in the design of a future electron-ion collider ring [6]. As such, an expansion of the existing NOECO technique to correct for the harmonic sextupoles would be useful due to their common, integral use in current and future accelerator design. In the National Synchrotron Light Source II (NSLS-II) ring [7], the number of harmonic sextupoles is greater than the number of chromatic sextupoles (180:90). Therefore, correcting harmonic sextupole errors is important for improving machine performance due to their greater influence. In this paper, we outline our expansion on the capabilities of existing sextupole correction techniques to accommodate for the harmonic sextupoles.

Some straightforward methods for calibrating harmonic sextupoles for correction would be (1) to temporarily convert them to chromatic ones; (2) to generate local orbit bumps through the sextupoles being calibrated. They are not practical when considering the limitations of routine operations of user facilities.

NONLINEAR OPTICS ON HYBRID DISPERSIVE ORBIT

When a sextupole sees vertical dispersion, its Hamiltonian reads as

$$H = \frac{p_x^2 + p_y^2}{2(1+\delta)} + \frac{K_2}{3}[x^3 - 3x(y + \eta_y\delta)^2], \qquad (1)$$

which includes a skew quadrupole component $2K_2\eta_y\delta \cdot xy$, with η_y the vertical dispersion, δ the beam momentum deviation, and sextupole strength $K_2 = \frac{1}{(B\rho)_0}\frac{\partial^2 B_y}{\partial x^2}$, normalized with the beam rigidity $(B\rho)_0$. Therefore, the nonlinear optics on off-energy orbits depend on the sextupole gradient, which can be utilized for their calibration and correction. A vertical dispersive wave can be generated through chromatic skew quadrupoles. In most light source rings, skew quadrupoles are widely equipped to control the residual vertical dispersion and linear coupling. Usually, a considerable amount of vertical dispersion can be generated, but only introduces weak coupling when the Betatron tune has sufficiently deviated from the linear difference/sum resonance. Thus, the nonlinear off-energy optics depends on not only chromatic sextupoles, but also on the original harmonic ones. In other words, horizontal harmonic sextupoles are converted into vertical chromatic ones, which makes their calibration and correction possible on hybrid dispersive orbits. In our studies, the NSLS-II ring double-bend achromat lattice was used to demonstrate these expanded capabilities.

At the NSLS-II ring, each odd-numbered cell is equipped with one 0.2 m long chromatic skew quadrupole (see Fig. 1). Their maximum gradients are $g_1 = 0.35\,\mathrm{T}\cdot\mathrm{m}^{-1}$, which is limited by the capacity of their power supplies. Assuming we can double their gradients to $g_1 = 0.70\,\mathrm{T}\cdot\mathrm{m}^{-1}$, a vertical dispersion wave with a ~ 0.1 m amplitude can be generated. The necessity for a double gradient is to increase the sensitivity of the nonlinear optics distortion to sextupoles. Although these gradients are twice as large as the maximum output of their power supplies, they are still quite weak compared to other operational quadrupoles with a maximum gradient of

* Work supported by US DOE Office of Science under Contract No. DE-SC0012704 operated by BNL
† yli@bnl.gov

ISBN: 978-3-95450-224-0 ISSN: 2673-7035 doi:10.18429/JACoW-FLS2023-TU1B3

$g_{1,max} = 22\,\mathrm{T}\cdot\mathrm{m}^{-1}$. Under these conditions, the exact coupled optics computed with the Ripken parameterization [8,9] indicates that the linear optics remain weakly coupled. In Fig. 1, the non-dominating functions $\beta_{1,y}$ and $\beta_{2,x}$ (dashed lines) are observed as very close to zero, while the dominating $\beta_{1,x}$ and $\beta_{2,y}$ (solid lines) are almost the same as in the uncoupled case. The skew quadrupoles also cause a small amount of horizontal dispersion to be leaked into the straight sections. Although such small residual dispersion could not be solely used to measure the off-energy nonlinear optics, its effect is accounted for in our method because the exact parameterization has been used.

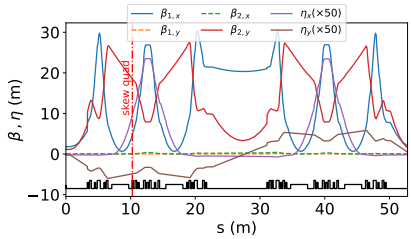

Figure 1: Coupled Twiss functions for a supercell at NSLS-II when a vertical dispersion wave is generated with chromatic skew quadrupoles. The location of the skew quadrupole is marked with a red vertical dash-dot line. Two non-dominating β-functions (dashed lines) indicate that this optics configuration remains weakly coupled.

For demonstration purposes, we choose a harmonic sextupole "SH3" and a chromatic sextupole "SM1" to compute their linear dependence on the off-energy optics, i.e., the so-called response vectors, as seen below. Only two dominating optics functions $\frac{d\beta_{1,x}}{d\delta}$ and $\frac{d\beta_{2,y}}{d\delta}$ observed at their corresponding BPMs were computed with the code MAD-X: PTC module [10] and verified with ELEGANT [11]. If no skew quadrupoles are used to excite the beam, they become the uncoupled β_x and β_y. The response vectors computed with and without the vertical dispersion are compared in Fig. 2. With horizontal dispersion, the dependence of off-energy optics on "SH3(N)" is not measurable in both the horizontal and vertical planes. On the hybrid dispersive orbits, a measurable dependence on "SH3(Y)" can be observed. Note that, for both cases, the dependence of the chromatic "SM1(Y/N)" is always measurable because it sees a large horizontal dispersion. In the meantime, the dependencies are quite similar since the optics are only slightly altered.

SIMULATIONS

In this simulation, random distributed errors on all 180 harmonic sextupoles are introduced and the distortion of off-energy optics are computed by comparing against the ideal lattice model. Then the needed sextupole correction scheme is obtained by the least squares regression,

$$\Delta\frac{d\beta}{d\delta} \approx M_{x,y}\Delta K_2, \qquad (2)$$

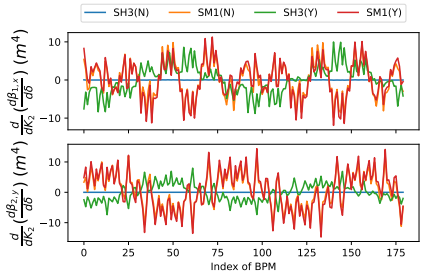

Figure 2: Comparison of the off-energy optics dependence on a chromatic sextupole "SM1" and a harmonic sextupole "SH3". With horizontal dispersion, the optics dependence on the harmonic sextupole (labeled as "SH3(N)") is too small to measure. On hybrid dispersive orbits, a measurable dependence (labeled as "SH3(Y)") is observed.

Here $M_{x,y}$ are the response matrices, which were obtained by computing the derivatives $d\beta/d\delta$ by varying sextupoles sequentially. For comparison, the optics distortions before and after correction, and the real error distributions and computed correction scheme are illustrated in Figs. 3 and 4, respectively. As seen in Fig. 4, the obtained correction schemes only approximately follow the real errors that were added in advance. This is due to the strong degeneracy that exists among sextupoles in the NSLS-II lattice.

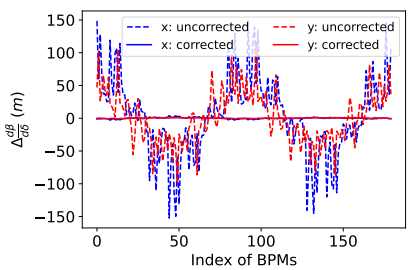

Figure 3: Distortions of the nonlinear optics with 180 randomly added errors. The dashed lines are uncorrected distortions, and the solid lines represent the distortions after correction.

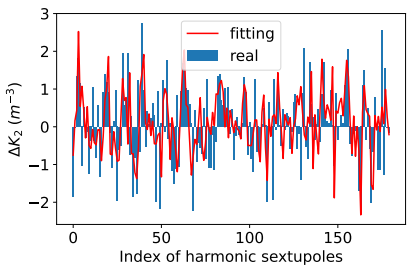

Figure 4: Comparison of the added errors (labeled as "real") on 180 harmonic sextupoles and the obtained correction scheme (shown with red lines labeled as "fitting").

ISBN: 978-3-95450-224-0 ISSN: 2673-7035 doi:10.18429/JACoW-FLS2023-TU1B3

The correction scheme based on the BPM observations can partially correct the optics distortion, therefore improve the dynamic aperture. To illustrate this, the dynamic apertures of the ideal machine, and uncorrected/corrected nonlinear lattices for the 2^{nd} simulation were computed for comparison (Fig. 5). Although the degraded dynamic aperture due to sextupole errors could not be fully recovered through the correction scheme, a significant improvement was achieved. Such improvement is the main purpose of calibrating and correcting the distorted nonlinear optics. If we could distinguish between the degeneracy among the sextupoles, further improvement could be made. This topic is slightly beyond the scope of this paper, however, but worth more study.

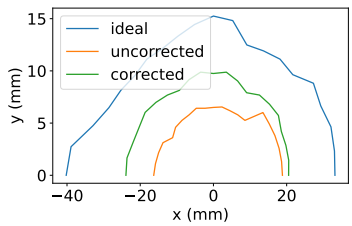

Figure 5: Comparison of the dynamic apertures for the ideal, uncorrected and corrected nonlinear lattices.

EXPERIMENTAL STUDIES

A two-stage proof-of-principle through beam-based calibration of sextupole errors was implemented at the NSLS-II storage ring. As the sextupoles are powered in series, the sextupoles lack individual configurability. Therefore, no actual nonlinear optics correction can be implemented with these limitations. For stage-1, we calibrated 90 chromatic sextupoles with with a similar technique like NOECO. First, spurious vertical dispersion was minimized using 15 chromatic skew quadrupoles, and the global linear coupling was well corrected with another 15 non-dispersive skew quadrupoles. The β seen by the BPMs were measured [12], then $\frac{d\beta}{d\delta}$ on horizontal dispersive orbits through varying the beam energy (i.e., RF frequency). By comparing the measured nonlinear optics against the design model, the chromatic sextupole errors (red bars in Fig. 6) were obtained using the model response matrices, and then incorporated into the lattice model. The updated model would be used as the reference for the stage-2 calibration.

For stage-2, a vertical dispersion wave was generated with 15 dispersive skew quadrupoles to their maximum capacity. Based on the measured dispersion, the 15 skew quadrupole settings and the vertical dispersion at the BPMs were reproduced with the lattice model as illustrated in Fig. 7. To achieve greater accuracy, a large amplitude vertical dispersion wave is preferred. However, it is limited by the capacity of the skew quadrupole power supply. Under the current configuration, ~ 0.05 m is the maximum amplitude that can be generated. The $\frac{d\beta}{d\delta}$ seen by the BPMs were re-measured, but from hybrid dispersive orbits this time. With the updated lattice model (incorporated with skew quadrupoles and chromatic sextupole errors) as the new reference, 180 harmonic sextupole errors were obtained (blue bars in Fig. 8).

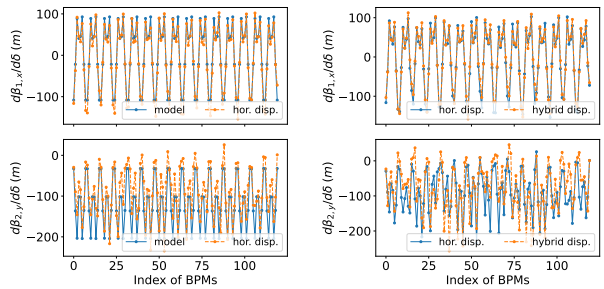

Figure 6: Off-energy optics at two stages. Left: off-energy optics of the ideal model and measurements from horizontal dispersive orbits. Bottom: measured optics from horizontal and hybrid dispersive orbits for harmonic sextupole calibration.

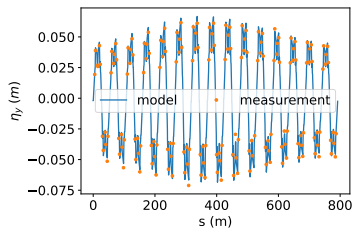

Figure 7: Vertical dispersion seen by the BPMs, and its reproduction with the lattice model.

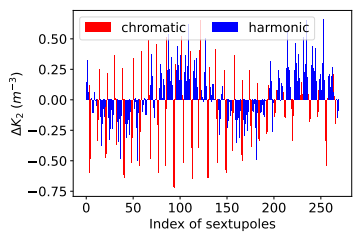

Figure 8: Sextupole errors from the two-stage measurements. The chromatic sextupoles marked with red bars are from the first stage, while the harmonic ones (blue bars) are from the second stage.

When the skew quadrupole polarities are flipped, the vertical dispersion pattern is flipped as well. It turns out that that the off-energy optics dependence on sextupoles in the flipped vertical dispersive orbit remains unchanged when the Ripken parameterization is used. This was used as the validation of the stage-2 measurement. More details can be found in the Ref. [13].

ISBN: 978-3-95450-224-0 ISSN: 2673-7035 doi:10.18429/JACoW-FLS2023-TU1B3

ACKNOWLEDGMENTS

We would like to thank the collaborative and productive discussion with Dr. D. Olsson, Prof. Y. Hao, Dr. J. Choi, Dr. Y. Hidaka, Dr. M. Song, Dr. G. Tiwari, Dr. X. Yang, et al.

REFERENCES

[1] R. Bartolini *et al.*, "Correction of multiple nonlinear resonances in storage rings", *Phys. Rev. Spec. Top. Accel. Beams*, vol. 11, no. 10, p. 104002, 2008. doi:10.1103/PhysRevSTAB.11.104002

[2] A. Franchi *et al.*, "First simultaneous measurement of sextupolar and octupolar resonance driving terms in a circular accelerator from turn-by-turn beam position monitor data," *Phys. Rev. Spec. Top. Accel. Beams*, vol. 17, p. 074001, 2014. doi:10.1103/PhysRevSTAB.17.074001

[3] D. Olsson *et al.*, "Nonlinear optics from off-energy closed orbits", *Phys. Rev. Accel. Beams*, vol. 23, p 102803, 2020. doi:10.1103/PhysRevAccelBeams.23.102803

[4] S. M. Liuzzo *et al.*, "Lifetime correction using fast-off-energy response matrix measurements", in *Proc. IPAC'22*, Bangkok, Thailand, Jun. 2022, pp. 1409–1411. doi:10.18429/JACoW-IPAC2022-TUPOMS008

[5] C. Sun *et al.* "Optimization of the ALS-U storage ring lattice" in *Proc. IPAC'16*, Busan, Korea, May 2016, pp. 2959–2961. doi:10.18429/JACoW-IPAC2016-WEPOW050

[6] Y. Cai *et al.*, "Optimization of chromatic optics in the electron storage ring of the electron-ion collider", *Phy. Rev. Accel. Beams*, vol 25, p. 071001, 2022. doi:10.1103/PhysRevAccelBeams.25.071001

[7] S. Dierker, "NSLS-II preliminary design report", Brookhaven National Lab, Upton, NY, USA, Tech. Rep. BNL-94744-2007, Nov. 2007.

[8] I. Borchardt *et al.*, "Calculation of beam envelopes in storage rings and transport systems in the presence of transverse space charge effects and coupling," *Zeitschrift für Physik C Particles and Fields*, vol. 39, p. 339, 1988. doi:10.1007/BF01548283

[9] F. Willeke and G. Ripken, "Methods of beam optics", in *AIP Conf. Proc,*, vol. 184, no. 1, pp. 758–819, 1989. doi:10.1063/1.38050

[10] F. Schmidt, "MAD-X PTC integration", in *Proc. PAC'05*, TN, USA, 2005, pp. 1272–1274, paper MPPE012. doi:10.1109/PAC.2005.1590731

[11] M. Borland, "elegant: A flexible SDDS-compliant code for accelerator simulation", Advanced Photon Source, Argonne National Lab, IL, USA, Tech. Rep. LS-287, 2000.

[12] P. Zisopoulos, Y. Papaphilippou, A. Streun, and V. G. Ziemann, "Beam optics measurements through turn by turn beam position data in the SLS", in *Proc. IPAC'13*, Shanghai, China, May 2013, paper WEPEA067, pp. 2663–2665.

[13] Y. Li *et al.*, "Nonlinear optics from hybrid dispersive orbits", arXiv preprint, arXiv:2303.03930, 2023. doi:10.48550/arXiv.2303.03930